

Supporting information

Achieving Direct Z-scheme Charge Transfer through Constructing 2D/2D α -Fe₂O₃/CdS Heterostructure for Efficient Photocatalytic CO₂ Conversion

Liyuan Long^{1,2,†,}, Gangyang Lv^{1,‡}, Qiutong Han², Xianchen Wu¹, Yu Qian¹, Dunhui*

Wang^{1,}, Yong Zhou^{2,*}, and Zhigang Zou^{2,*}*

¹ Micro-Electronics Research Institute and School of Electronics and Information,

Hangzhou Dianzi University, Hangzhou 310018, China

² National Laboratory of Solid State Microstructures and Department of Physics,

Nanjing University, Nanjing 210093, China

Email: liyuan-long@hdu.edu.cn; wangdh@hdu.edu.cn; zhouyong1999@nju.edu.cn;

zgzou@nju.edu.cn

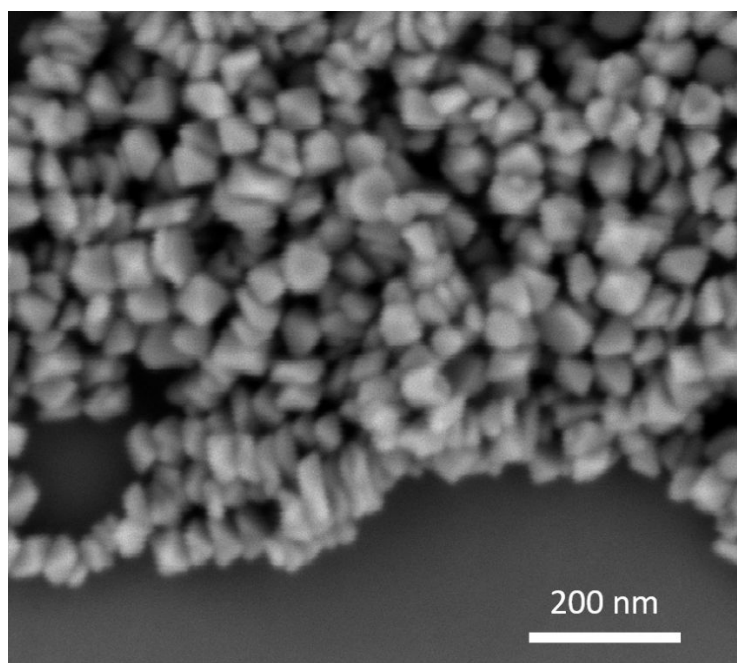


Figure S1. The FESEM image of α -Fe₂O₃ nanoparticles fabricated under the precursor solution with 1.4 ml water and without any other growth condition difference compared to α -Fe₂O₃ NSs.

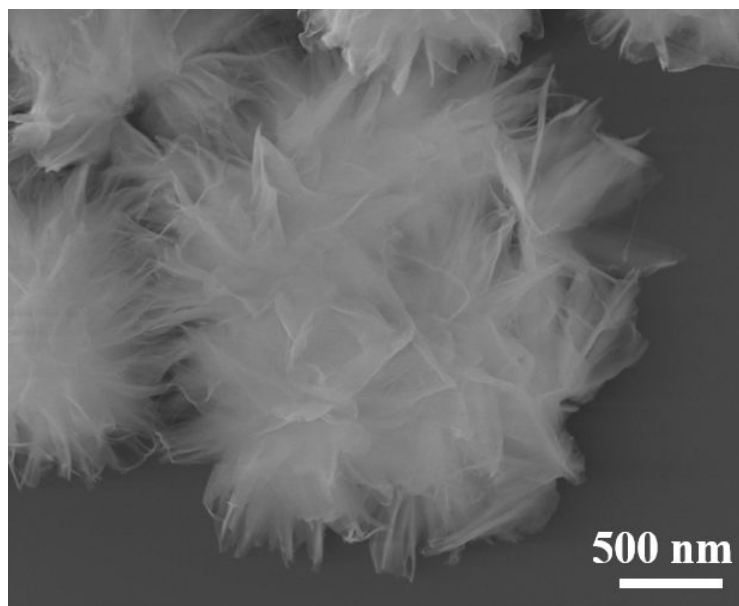


Figure S2. The FESEM image of pure CdS nanosheets. These CdS nanosheets interlace to each other and form hierarchical flower-like microsphere which is highly beneficial to expose their surface for interaction with α -Fe₂O₃ nanosheets.

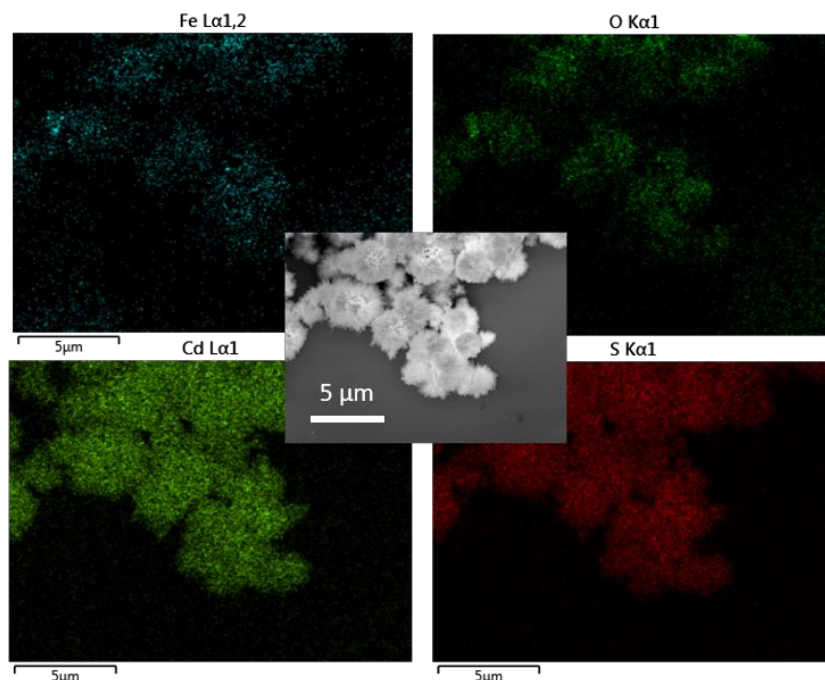


Figure S3. The EDX mappings of Fe, O, Cd, S elements and the corresponding FESEM image of large area of $\alpha\text{-Fe}_2\text{O}_3\text{@CdS}$ heterostructure. To obtain the EDX mappings, the corresponding FESEM image is acquired at 20 KV, leading to exhibiting hierarchical microspheres with relatively vague surface morphology. The distribution of Fe and O elements uniformly correspond to their morphology image as well as element distribution of Cd and S, effectively demonstrating the formation of homogenous $\alpha\text{-Fe}_2\text{O}_3\text{@CdS}$ heterostructure.

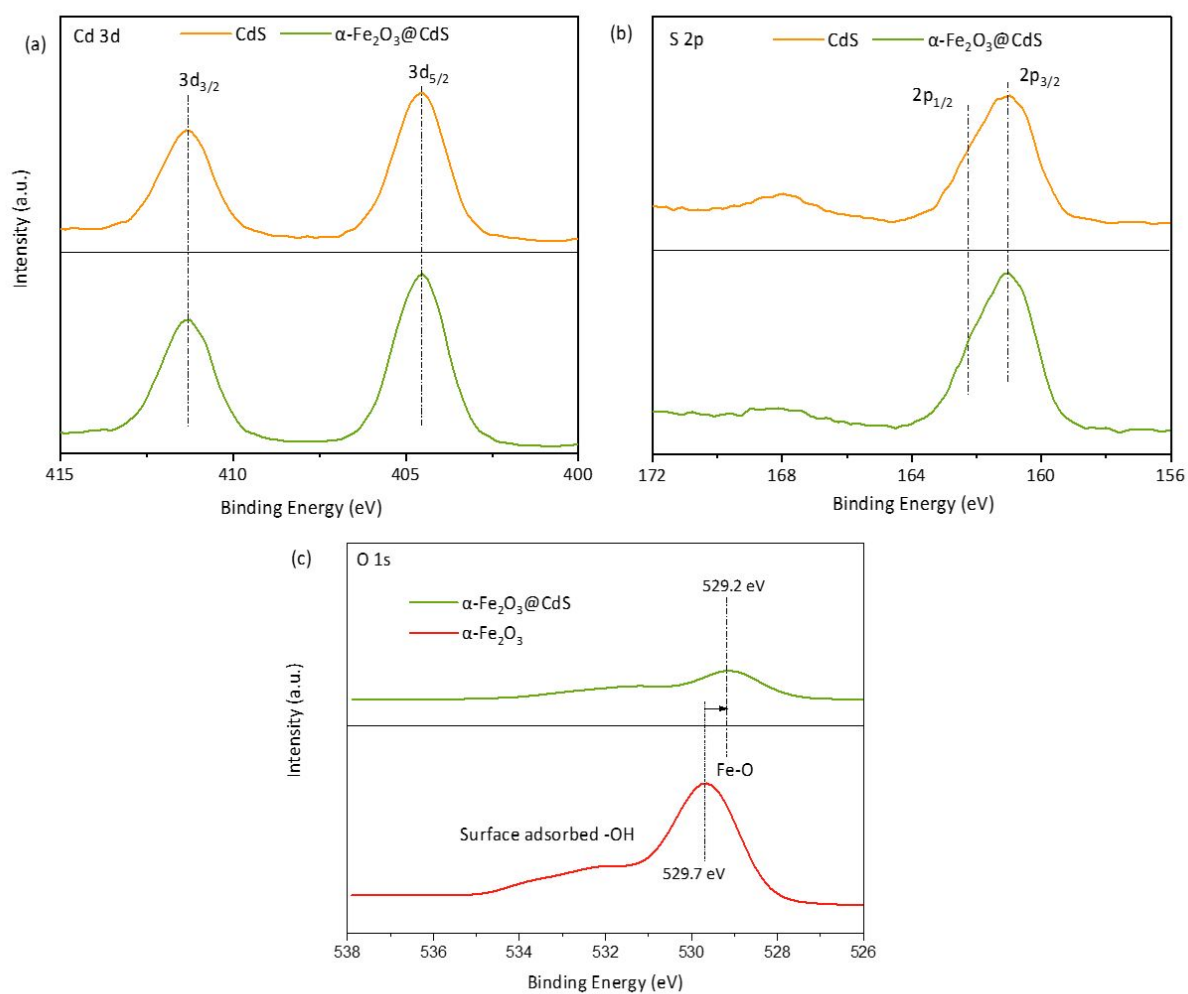


Figure S4. High-resolution XPS spectra of (a) Cd 3d, (b) S 2p and (c) O1s. The left shoulder of O1s XPS spectra should come from surface adsorbed hydroxyl.¹

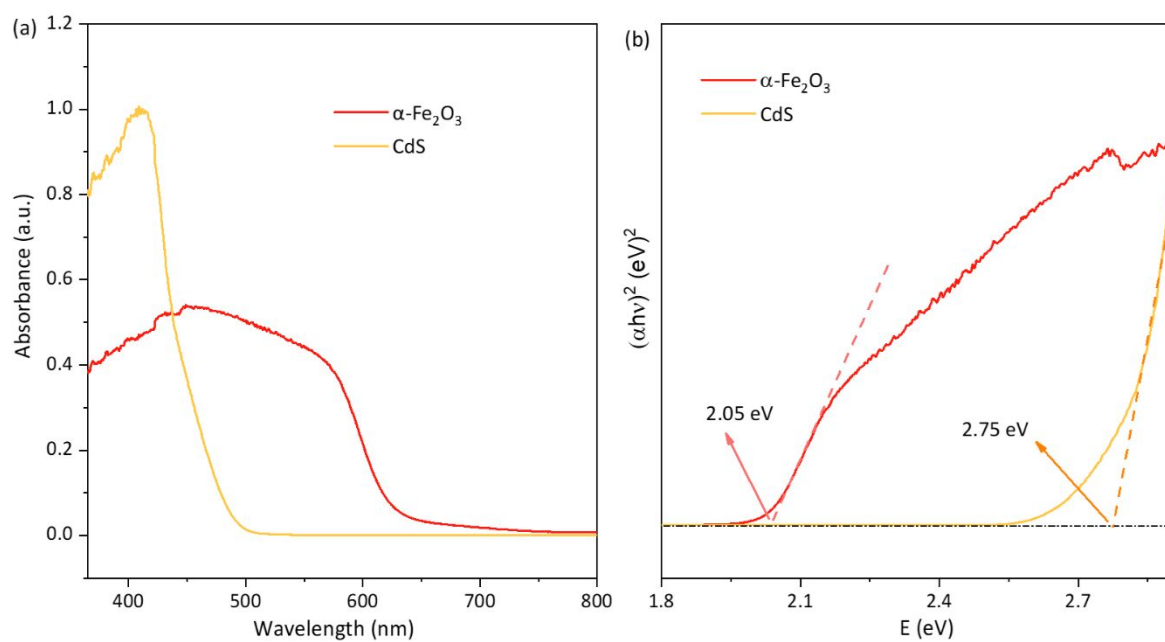


Figure S5. (a) UV-vis diffusive reflectance spectra of pure α -Fe₂O₃ NSs and CdS NSs.

(b) Tauc plots of direct-bandgap α -Fe₂O₃ and CdS converted from spectra in [Figure](#)

[S5a](#) according to Kubelka-Munk functions.

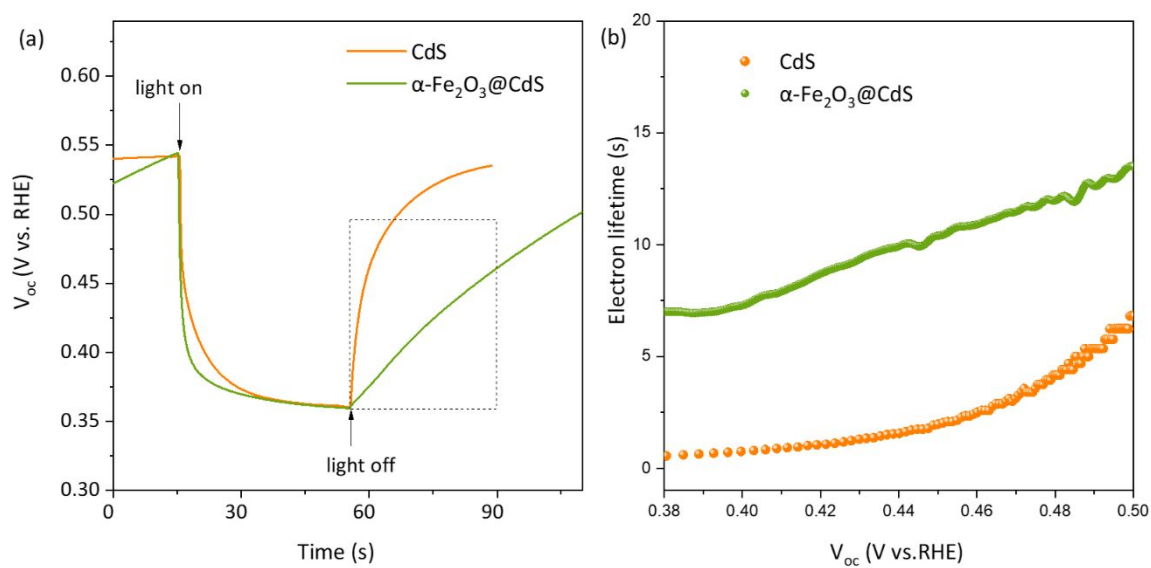


Figure S6. (a) Transient open circuit potential plots under simulated solar light-switching. (b) The photoelectron lifetime under different potential converted from the decay dynamics of V_{oc} at the moment of light off.²⁻³

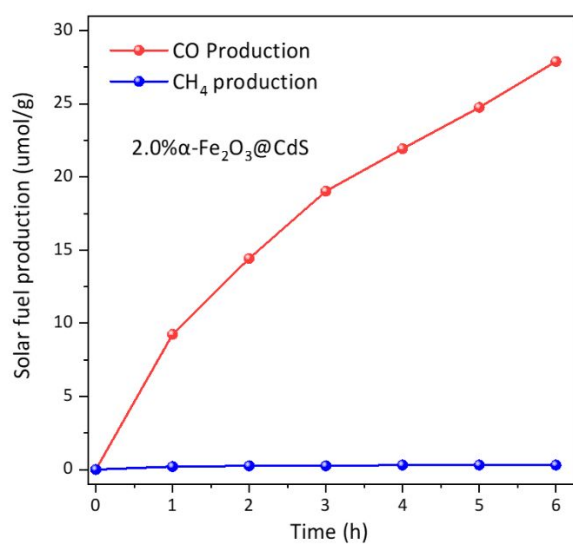


Figure S7. Comparison of CO and CH₄ production of photocatalytic CO₂ conversion for 2% α -Fe₂O₃@CdS heterostructure. The negligible CH₄ production which is beyond the detection accuracy of gas chromatograph reflects the high product selectivity of α -Fe₂O₃@CdS photocatalyst for CO₂ conversion.

REFERENCES

- [1] Pan, J.; Guo, F.; Sun, H.; Li, M.; Zhu, X.; Gao, L.; Shi, W. Nanodiamond Decorated 2D Hexagonal Fe₂O₃ Nanosheets with a Z-Scheme Photogenerated Electron Transfer Path for Enhanced Photocatalytic Activity. *J. Mater. Sci.* **2021**, *56*, 6663-6675.
- [2] Yang, H.; Fan, W.; Vaneski, A.; Susha, A. S.; Teoh, W. Y.; Rogach, A. L. Heterojunction Engineering of CdTe and CdSe Quantum Dots on TiO₂ Nanotube Arrays: Intricate Effects of Size-Dependency and Interfacial Contact on Photoconversion Efficiencies. *Adv. Funct. Mater.* **2012**, *22*, 2821-2829.

[3] Bang, J. H.; Kamat, P. V. Solar Cells by Design: Photoelectrochemistry of TiO_2

Nanorod Arrays Decorated with CdSe. *Adv. Funct. Mater.* **2010**, *20*, 1970-1976.